



## Trends in the surface UV radiation at the Polish Polar Station, Hornsund, Svalbard (77°00' N, 15°33' E), based on the homogenized time series of broad-band measurements (1996-2016) and reconstructed data (1983-1995)

5 Janusz W. Krzyścin<sup>1</sup>, Piotr Sobolewski<sup>1</sup>

<sup>1</sup>Institute of Geophysics, Polish Academy of Sciences, Warsaw, 01-452, Poland

Correspondence to: Janusz W. Krzyścin ([jkrzys@igf.edu.pl](mailto:jkrzys@igf.edu.pl))

**Abstract.** Erythemal daily doses measured at the Polish Polar Station, Hornsund (77°00'N, 15°33'E), for the period 1996-2001 and 2005-2016 are homogenized using yearly calibration constants derived from the comparison of observed doses for cloudless conditions with the corresponding doses calculated by radiative transfer (RT) simulations. Modeled all-sky doses are calculated by the multiplication of cloudless RT doses by the empirical cloud modification factor dependent on the daily sunshine duration. An all-sky model is built using daily erythemal doses measured in the period 2005-2006-2007. The model is verified by comparisons with the 1996-1997-1998 and 2009-2010-2011 measured data. The daily doses since 1983 (beginning of the proxy data) are reconstructed using the all-sky model with the historical data of the column ozone from the satellite measurements (SBUV merged ozone data set), the snow depth (for ground albedo estimation), and the observed daily sunshine duration at the site. Trend analyses of the monthly and yearly time series comprising of the reconstructed and observed doses reveal statistically significant trend only in March (~1%/yr) in the period 1983-2016. The trends based on the observed data only (1996-2001 and 2005-2016) show declining tendencies during spring (March-April-May) of ~1%/yr. An analysis of sources of the yearly dose variability since 1983 provides that cloud cover changes are a basic driver of the long-term UV changes at the location.

### 1 Introduction

The importance of the solar UV radiation on human health and ecosystems is widely discussed in the literature since the ozone hole discovery in the early 1980s (e.g. WMO, 2014). The Montreal Protocol was signed by UN countries in 1987 to protect the ozone layer, which acts as a shield against the solar UV. Since 1980 especially large ozone depletion was observed every year in the late winter and spring, the so-called ozone hole, over Antarctica (e.g. WMO, 2014). However, the ozone hole over the Arctic was observed only once in 2011 (Garcia, 2011; Bernhard et al., 2013). The ozone downward



trend and the increase of the surface UV in the Arctic was observed in 1990s (Fioletov et al., 1997; Newmann et al., 1997; Gurney, 1998).

The amount of column ozone and its vertical distribution have been measured using a ground-based and satellite network.

Nowadays, the ozone distribution over the whole globe is available for scientific purposes. The surface UV radiation in the

5 UV-B range also depends on the Sun's elevation, cloud/aerosol characteristics, and the surface albedo, which are widely variable from site to site. There are a limited number of ground-based stations measuring erythemally effective doses continuously for longer than 20 years. These include only 5 northernmost stations above 70° N: Alert (82.5° N, 62.31° E), Ny-Ålesund (78.92° N, 11.92° E), Hornsund (77.0° N, 15.33° E), Resolute (74.72° N, 94.98° W, and Barrow (71.32° N, 156.68° W). The algorithm to calculate the surface UV using the satellite data (total ozone, ground-reflectivity) over high-  
10 latitude regions sometimes failed due to the fact that the observed high reflectivity surfaces might be erroneously classified as high ground-albedo (from snow and ice cover) or cloud effect (Tanskanen et al. 2007). It is crucial to examine the UV variability over the Arctic regions, especially for high latitudinal coastal sites, because of rich and diverse ecosystems located in this area (Hessen et al, 2001). It is anticipated that anthropogenic climate effects will be the most pronounced in high latitudinal regions (Taalas et al., 2000; IPCC 2014).

15 Maintaining homogeneity of long-term UV time series (20+yr) taken from various instruments is a challenging task especially for remote sites. In this paper, we propose a method for the UV data homogenization applicable for any remote Arctic site like the Polish Polar Station Hornsund (Section 2 and 3). Next, we reconstruct the UV doses dating back to 1983 when the observations of proxies for the UV variability started at Hornsund (Section 4). Finally, we search for linear trends in monthly and yearly doses (Section 5) separately for the periods comprising both the reconstructed and observed data  
20 (1983-2016) and for the observed data only (1996-2016 with the 2002-2004 gap).

## 2 UV and ancillary data

The erythemal UV measurements at Hornsund were carried out since 1996 up to 2001 by an improved version (with

temperature stabilization) of the classic Robertson-Berger UV meter. This was a prototype of the presently widely used broadband Solar Light Model 500 (denoted SL 500) radiometer produced by Solar Light Co. RB meter was designed in the

25 early 1970s to measure erythemal solar irradiation as its spectral characteristics resembled that of the human skin (McKinlay and Diffey, 1987). The prototype was designed in the Institute of Geophysics (IG), Polish Academy of Sciences (PAS), Belsk, in the late 1980s and since then took part in the UV monitoring at the Central Geophysical Laboratory, IG PAS, Belsk, Poland. It was moved to the Hornsund observatory in 1995 and put into regular UV monitoring in 1996 (Krzyżcin and Sobolewski, 2001) that lasted up to autumn 2001. Since spring 2004, a new UV broadband meter Kipp and Zonen UVS-AE-T (Fig. 1) has been installed at Hornsund and started continuous UV monitoring in April 2005. During the two years of its  
30 operation (2006-2007) it was calibrated by the IG PAS substandard Kipp & Zonen UVS-AE-T (No. 616), which was



frequently calibrated against the Belsk's Brewer spectrophotometer (Sobolewski and Krzyścin, 2006). There were logistical difficulties with the calibration of the Hornsund meter by a higher-level standard (e.g. the Brewer spectrophotometer) as the station could be reached only by snowmobiles (in spring), helicopters or ships (in summer). Thus, we decided to apply radiative transfer (RT) model simulations for clear-sky conditions to calibrate the output of the biometer during cloudless days and perform a homogenization of the past UV data.

The following ancillary data routinely measured at Hornsund is used in the model simulations: snow depth, cloud fractions by low-, mid-, and high-level clouds, aerosols characteristics (aerosols optical depth, single scattering albedo from the Cimel Sunphotometer observations since 2004), and sunshine duration (by a Campbell-Stokes recorder).

### 3 Data Homogenization

Clear-sky conditions over the Hornsund observatory were identified by the examination of the 1-minute erythral irradiation daily pattern. The smoothness of the pattern and the steady increase (before local noon) and decrease (after local noon) of the irradiances provided a criterion for cloudless day. The Tropospheric Ultraviolet-Visible (TUV) RT model by Madronich (1993) is implemented to calculate hypothetical clear-sky daily dose for the selected cloudless days. The TUV input consists of the column ozone amount (taken from the site overpasses by the Solar Backscatter Ultraviolet (SBUV) instrument onboard the NOAA satellites, aerosols characteristics from the AERONET database (aerosol optical depth, single scattering albedo of aerosols, and asymmetry factor). The ground albedo in UV range is approximated by a local formula:

$$Albedo_{GROUND} = 0.1 + Depth_{SNOW}/40, \quad (1)$$

where  $Depth_{SNOW}$  is the measured snow depth in cm, for  $Depth_{SNOW} > 32$  cm.  $Albedo_{GROUND} = 0.9$ . Equation (1) was found experimentally, to have the best agreement with the measured daily doses in the period when the UV data at Hornsund were calibrated by the IG PAS substandard (2006-2007).

For each year (2005-2016) ratios between the modeled and observed daily doses were averaged to provide the annual correction factor, which is consequently applied to the measured all-sky daily doses. The annual correction factor (ACF) was calculated separately for selected ranges of the noon solar zenith angle (SZA);  $SZA \leq 60^\circ$ ,  $60^\circ < SZA \leq 70^\circ$ ,  $70^\circ < SZA \leq 80^\circ$ , and  $SZA > 80^\circ$ . Figure 2 shows ACF time series (2005-2016) for four SZA ranges. It is worth noting that ACF oscillates in the range 0.95-1.05 for  $SZA \leq 60^\circ$ ,  $60^\circ < SZA \leq 70^\circ$ . There is a much larger ACF variability of ~0.75-1.35 for  $SZA > 80^\circ$  (February – 15 March, October), i.e. for a period with a weak UV intensity when the solar UV is dominated by the diffusive component related to aerosol characteristics, which sometimes is not well parameterized in the RT model. All time series shown in Fig.2 are trendless. It seems that the biometer's sensitivity to the UV radiation is constant since 2005, i.e. there is no need to use any correction for the instrument aging and  $ACF=1$ . The same procedure was used for the first period (1996-2001) of the UV monitoring at Hornsund but constant aerosols of AOD at 340 nm equal to 0.16 was assumed (no Cimel



sunphotometer observations in that period). Moreover, only one ACF value was calculated regardless of SZA. Following ACF values were applied to the observed daily dose: 1.00 (1996), 1.20(1997), 1.40(1998), 1.79 (1998), 1.80 (1999), 2.00 (2000), and 2.50 (2001).

#### 4 Data Reconstruction

5 Reconstruction of the erythemal daily doses is based on a regression model using proxies for the cloud attenuations i.e. a cloud cover observed by the technical staff and a sunshine duration measured by a Campbell-Stokes recorder. Model's regression parameters were determined using the 2005-2006-2007 daily erythemal doses (by Kipp and Zonen UV biometer). The model is verified using the 1996-1997-1999 data (output of SL 500 prototype) and 2009-2010-2011 (output of Kipp and Zonen biometer).

10 A semi-empirical model is built to reproduce the measured daily doses (erythemal  $\text{Jm}^{-2}$ ) for the period 2006-2007-2008.

$$Dose(t) = CMF(t) \times Dose_{\text{CLEAR-SKY}}(t), \quad (2)$$

where  $Dose_{\text{CLEAR-SKY}}(t)$  is a hypothetical clear-sky daily dose in day  $t$  from the radiative transfer model simulations (TUV) with the following input:

- the daily total ozone ( $\text{TO}_3$ ) from the station satellite overpasses (SBUV merged data set)
- 15 - the snow albedo according formula (1) with the snow depth from the station meteorological data
- daily observed aerosol optical depth (AOD) values by the Cimel sunphotometer or the long-term (2004-2014) monthly means of AOD at 340 nm (0.16) if there were no CIMEL measurements at the station.

$CMF$  is an empirical cloud modification factor (CMF) used to parameterize an attenuation of hypothetical clear-sky daily doses by clouds. Various combinations of regressors (explaining variables) were examined using standard multi-linear regression to reproduce observed erythemal doses. These included the cloud cover (by total, low-, mid-, and high-level clouds), cloud types identified by an observer (every 3 h), and the measured daily relative sunshine duration (the sunshine duration divided by the pertaining day length). The time series of these regressors were available since 1983. Finally, the relative sunshine duration,  $SUN\_DUR(t)$ , was selected as the best regressor and the following formula was obtained:

$$CMF(t) = 1.0324 [SUN\_DUR(t)]^{0.1951}, \quad (3)$$

25 Model (3) explains ~45% of CMF variance. The regression coefficients (1.0324, 0.1951) are found highly statistically significant at the 99% confidence level. It appeared that the cloud fractions and types were not good predictors due to the large variability of cloud types with different optical properties. Moreover, cloud observations at the station were taken every 3 h and the closest observation to the noon was 12 GMT, i.e. approximately 1 h after the local noon. Model (2) with CMF defined by Eq. (3) performs almost perfectly (see Fig.3a). The model-observation correlation coefficients exceed 0.9 and the



smoothed pattern of scattered data obtained by LOWESS (locally weighted scatterplot smoothing, Cleveland, 1979) matches the 1-1 line (perfect agreement line - diagonal of the square).

The regression coefficient of models (2) was computed using the multi-linear least-squares fit to the observed 2005-2006-2007 daily doses. Comparisons of the modeled data to the observed ones taken in different periods will provide a kind of the model's verification and will support a correctness of the calibration constants applied to total UV data (Section 3). Figure 3b and Figure 3c show the comparisons for the period 2009-2010-2011 and 1996-1997-1998, respectively. The model-observation correlation coefficients are high (~0.95) and the smoothed patterns of scattered data points match the 1-1 line (perfect agreement line) throughout the whole range of the data variability.

The model-observation agreement appears even better for the monthly averages of daily erythemal doses (Fig.3d) for three periods together: 1996-1997-1998, 2005-2006-2007, and 2009-2010-2011. Here the correlation coefficient is equal to ~0.99 and the linear regression line has the slope of 1.002. Thus, the simple parameterization of cloud effects on the surface erythemal dose by Eq. (3) could be used for a reconstruction of the long-term UV variability at Hornsund. Moreover, almost the same model performance was found for the periods with the UV observations done by different instruments: 1996-1997-1998 (SL 500 prototype), 2005-2006-2007 (model's built period) and 2009-2010-2011 (Kipp and Zonen UVS-AE-T radiometer). It supports the data homogeneity of the UV observations by different biometers since 1996.

## 5 Results

The monthly mean erythemal doses from the UV observations (1996-2001, and 2005-2016) and reconstructed by the model (2) for the period 1983-1995, and the period 2002\_2004 is used to estimate the long-term variability and linear trends for the whole 1983-2016 period and for the 1996-2016 period (with the gap in the period 2002-2004) using only the ground-based data.

Figure 4 illustrates the time series of the monthly (March-September) and yearly fractional deviations,  $FD\_DOSE(t)$ , i.e. deviations from the long-term (1996-2016) monthly means,  $\langle DOSE(t) \rangle$ , in percent of the long-term means:

$$FD\_DOSE(t) = (DOSE(t) - \langle DOSE(t) \rangle) / \langle DOSE(t) \rangle * 100\%, \quad (4)$$

There are large year-to-year fluctuations in the monthly fractional deviations in the range between -40% and 40%. The smoothed data patterns show: an increasing tendency throughout the whole period in March and April, the trendless behavior in July and September, the increase/decrease in May and June with the turning point around 1996, the decrease/increase in August with the turning point around 1998. Yearly sums of the erythemal daily doses show increasing tendency of about 1% per year up to ~1996 and afterward a leveling off.

Table 1 shows the linear trend values by the least-squares regression. The trends are calculated for the period 1983-2016 (both observed and reconstructed data) and for the period 1996-2016 taking into account only the observed data. The



statistically significant (at  $2\sigma$  level) positive trend is found only in March ( $\sim 1\%$  per year) for the 1983-2016 period. The negative trends  $\sim 1\%$  per year are calculated in April, May, and June for the shorter period (since 1996). It seems that the negative trend in April was caused by two extremely high positive fractional deviations ( $\sim 30\text{-}40\%$ ) at the beginning of time series (1996 and 1997) and the trend in shorter period does not correspond with an increasing tendency found in the whole data period.

To find sources of the long-term behavior of total yearly dose,  $TYD(t)$ , we calculate the corresponding pattern for total ozone and the relative sunshine duration for the same period. The explained variables are weighted using the monthly weights according to participation of the monthly doses in  $TYD(t)$ , i.e.  $\{0.02, 0.10, 0.21, 0.27, 0.22, 0.12, 0.04\}$  for each month since March up to September, respectively. A multivariate regression of the  $TYD$  fractional deviations,  $FD\_TYD(t)$ , on the fractional deviations of the weighted total ozone,  $FD\_w\_TO_3(t)$ , and the weighted relative sunshine duration,  $FD\_w\_SUN\_DUR(t)$  is found as follows,

$$FD\_TYD(t) = -3.0304 - 0.7498 FD\_w\_TO_3(t) + 0.5017 FD\_w\_SUN\_DUR(t), \quad (5)$$

The Model (5) explains 63% of the total variance (Fig5.a) and provides that cloudiness changes were the dominant the factor of  $TYD$  variability.  $TO_3$  changes induced  $FD\_TYD(t)$  variability in the range  $\sim 1\%$ . It is worth mentioning that the weighted pattern of annual  $TO_3$  values shows full recovery of ozone in 2016. Clouds caused  $FD\_TYD(t)$  increase of  $\sim 3\%$  in the period 1983-1996 and 2008-2016, and a decrease of  $\sim 3\%$  in the period 1996-2003.

Previous studies showed that the sunshine duration was a worse proxy for a parameterization of the cloud attenuation when compared to the total solar (300-3000nm) radiation. It does not reflect basic cloud characteristics such as cloud fractions and the cloud optical thickness (Koepke et al., 2006). The total solar radiation was measured at Hornsund in some disjointed periods since 1983 but the data was not calibrated by a higher-ranking instrument. Thus, we decided to use only sunshine duration data to parameterize the cloud effects since 1983 at Hornsund. Sunshine duration measurements by a Campbell-Stokes instrument seem to be less influenced by the instrument sensitivity lost and its calibration is very simple as during cloudless conditions the sunburn track should appear throughout the whole day.

## 6 Discussion and Conclusions

A procedure for the examination of the UV data homogeneity is proposed based on RT simulations for clear-sky conditions. It allows introducing the yearly calibration coefficient showing the instrument sensitivity lost (1996-2001) and stable behavior in the period of measurements by the Kipp and Zonen UVS-AE-T biometer (2005-2016). For all-sky conditions, the regression model is built using 3-year data (2005-2006-2007) and comparisons of the modeled data with earlier (1996-1997-1998) and later (2009-2010-2011) data shows the same behavior as for the model building period that supports the data homogeneity and its usefulness for the long-term trend analysis. The regression model allows the UV dose reconstruction



since 1983, i.e. in the period when the daily total ozone (from the satellite observations) and the sunshine duration data, which represented a proxy for the cloud effects on surface UV, were both available. The reconstruction model is also used to fill the data gaps in the UV observing period (since 1996).

Analyses of the yearly doses at Hornsund reveal a non-statistically significant trend in the period 1983-2016. Two phases of the long-term behavior of total yearly doses could be identified, i.e. a positive tendency in total yearly doses in the period 1983-2000 and afterward a leveling off. The linear trend calculation by a standard least-squares fit applied to the measured monthly means (1996-2001 and 2005-2016) shows apparent declining tendency in April, May, and July. However, these trends are influenced by two-three years of high positive fractional deviations of the erythemal doses at the beginning of the shorter time series. Longer time series (since 1983) do not show any sign of the declining tendency, starting around 1996.

Bernhard et al. (2011) analysis of the monthly trends at Barrow (Alaska) for the period 1990-2010 revealed statistically significant trend only in October (decline of 1% per year) when the UV intensity was rather weak without the erythemal risk. The ozone effect on the surface UV appeared as a secondary source of the UV variability causing the long-term oscillations in the range of  $\pm 1\%$  in the period 1983-2016. Such total ozone pattern is not unique in the Arctic. Figure 6 shows the long-term (1979-2016) pattern of the total ozone mean (using SBUV merged data) for the period May-August at Belsk, Barrow, and Resolute, i.e. in the period of the year with naturally high UV radiation. The ozone forcing on the surface UV at these sites is weak since the beginning of the 1990s.

Cloud effects are the basic source of the UV variability at Hornsund. Here the relative sunshine duration was used as the proxy explaining the cloud effects. It allows to identify, for example, a decrease in cloudiness in the period 1983-2000 but the corresponding increase in the total yearly doses seems to be larger than that inferred from the proxy pattern. Evidently, the cloud optical thickness should be also responsible for the yearly UV variability.

It seems that the excessive UV radiation will be unlikely over the Arctic during the 21<sup>st</sup> century as prolonged decrease of ozone will not be possible due to the declining tendency in the concentration of the ozone-depleting chemicals in the stratosphere, anticipated intensification of the Brewer-Dobson circulation loading higher amount of ozone into the Arctic stratosphere (WMO, 2014). The downward UV tendency in the Arctic will be also induced by the increase in the cloudiness, and the lowering of the ground albedo due to the snow and sea-ice melting (e.g. Bais et al., 2015).

A continuation of UV measurements at Hornsund seems to be necessary as it is located in a region vulnerable to climate changes with the local climate strongly dependent on the heat arriving with the Gulf Stream. A projection of the weakening of the Atlantic Meridional Overturning Circulation (Boulton et al., 2014) will lead to the surface cooling at the location. It can not be excluded that high reflectivity areas (sea-ice and snow) will extend over west Svalbard and the present climatic contrast between west (warm) and east (cold) part of Svalbard will disappear. Any projection for erythemal irradiance by the end of the 21<sup>st</sup> century is the most uncertain for this part of the Arctic.



*Data Availability.* The total ozone overpass data was acquired from the data archive of SBUV merged ozone at <ftp://toms.gsfc.nasa.gov/pub/sbuv/MERGED/>. The sunshine duration and snow height at Hornsund were available at [https://github.com/AtmosIGFPAN/Hornsund\\_Data](https://github.com/AtmosIGFPAN/Hornsund_Data). Aerosols optical properties were taken from AERONET database at [https://aeronet.gsfc.nasa.gov/new\\_web/aerosols.html](https://aeronet.gsfc.nasa.gov/new_web/aerosols.html). Finally, the reconstructed and observed erythemal doses at Hornsund for the period 1983-2016 could be found at [https://github.com/AtmosIGFPAN/Hornsund\\_Data](https://github.com/AtmosIGFPAN/Hornsund_Data).

5

*Acknowledgments.* Funding for this study was provided by the Ministry of Science and Higher Education, Republic of Poland, within statutory activity No 3841/E-41/S/2017. We are grateful to the numerous dedicated individuals who have collected meteorological data for many decades.

10





## References

- Bais, A. F., McKenzie, R. L., Bernhard, G., Aucamp, P. J., Ilyas, M., Madronich, S., and Tourpali, K.: Ozone depletion and climate change: Impacts on UV radiation, *Photochem. Photobiol. Sci.*, 14, 19–52, 2015.
- Bernhard, G.: Trends of solar ultraviolet irradiance at Barrow, Alaska, and the effect of measurement uncertainties on trend detection, *Atmos. Chem. Phys.*, 11, 13029–13045, doi:10.5194/acp-11-13029-2011, 2011.
- 5 Bernhard, G., Dahlback, A., Fioletov, V., Heikkilä, A., Johnsen, B., Koskela, T., Lakkala, K., and Svendby, T.: High levels of ultraviolet radiation observed by ground-based instruments below the 2011 Arctic ozone hole, *Atmos. Chem. Phys.*, 13, 10573–10590, doi:10.5194/acp-13-10573-2013, 2013.
- Bernhard, G., Arola, A., Dahlback, A., Fioletov, V., Heikkilä, A., Johnsen, B., Koskela, T., Lakkala, K., Svendby, T., and J. Tamminen.: Comparison of OMI UV observations with ground-based measurements at high northern latitudes, *Atmos. Chem. Phys.*, 15, 7391–7412, doi: 10.5194/acp-15-7391-2015, 2015.
- 10 Boulton, C., Allison, L., Lenton, T.: Early warning signals of Atlantic Meridional Overturning Circulation collapse in a fully coupled climate model, *Nat. Commun.*, 5, 5752, doi:10.1038/ncomms6752, 2014.
- Cleveland, W.S.: Robust locally weighted regression and smoothing, *J. Am. Stat. Assoc.*, 74(368), 829–836, doi:10.2307/2286407, 1979.
- 15 Fioletov, V.E., Kerr, J.B., Wardle, D.I., Davies, J., Hare, E.W., McElroy, C.T., and Tarasick, D.W.: Long-term ozone decline over the Canadian Arctic to early 1997 from ground-based and balloon observations, *Geophys. Res. Lett.*, 24, 2705–2708, 1997.
- Garcia, R.R.: An Arctic ozone hole? *Nature*, 478, 462–463, 2011.
- 20 Gurney, K. R.: Evidence for increasing ultraviolet irradiance at Point Barrow, Alaska, *Geophys. Res. Lett.*, 25, 903–906, 1998.
- Hessen, D. O. (Ed.): *UV Radiation and Arctic Ecosystems*, 321 pp., Springer-Verlag, New York, 2001.
- IPCC (Intergovernmental Panel on Climate Change), *Climate Change 2014 – Impacts, Adaptation and Vulnerability: Part B: Regional Aspects: Working Group II Contribution to the IPCC Fifth Assessment Report*. Cambridge: Cambridge University Press. doi:10.1017/CBO9781107415386, 2014.
- 25 Koepke, P., De Backer, H., Bais, A., Curylo, A., Eerme, K., Feister, U., Johnsen, B., Junk, J., Kazantzidis, A., Krzyscin, J., Lindfors, A., Olseth, J., Den Outer, P., Pribulova, A., Schmalwieser, A., Slaper, H., Staiger, H., Verdebout, J., Vuilleumier, L., Weihs, P.: Modelling solar UV radiation in the past: comparison of algorithms and input data, *Proc. SPIE 6362, Remote Sensing of Clouds and the Atmosphere XI*, 636215–636215-11, doi:10.1117/12.687682, 2006.
- 30 Krzyscin, J., Sobolewski, P.: The surface UV-B irradiation in the Arctic: observations at the Polish polar stations, Hornsund (77N,15E), 1996–1997, *J. Atmos-Sol. Terr. Phys.*, 63, 321–329, 2001.
- Madronich, S.: UV radiation in the natural and perturbed atmosphere, in *Environmental Effects of UV (Ultraviolet) Radiation* (M. Tevini, ed.), Lewis Publisher, Boca Raton, pp. 17–69, 1993.



- McKinlay, A. F. and Diffey, B. L.: A reference action spectrum for ultraviolet induced erythema in human skin, in: Commission International de l'Éclairage (CIE), Research Note, 6, No. 1, 17–22, 1987.
- Newman, P. A., Gleason, J. F., McPeters, R. D., and Stolarski, R. S.: Anomalous low ozone over the Arctic, *Geophys. Res. Lett.*, 24(22), 2689–2692, 1997.
- 5
- Sobolewski, P., Krzyścin, J.: UV measurements at the Polish Polar station, Hornsund, calibration and data for the period 2005–2006, *Publ. Inst. Geophys. Pol. Acad., Sc, D-67(382)*, 123–132, 2006.
- Taalas, P., Kaurola, J., Kylling, A., Shindell, D., Sausen, R., Dameris, M., Grewe, V., Herman, J., Damski, J., and Steil B.: The impact of greenhouse gases and halogenated species on future solar UV radiation doses, *Geophys. Res. Lett.*, 27(8), 1127–1130, 2000.
- 10
- Tanskanen, A., Lindfors, A., Määttä, A., Krotkov, N., Herman, J., Kaurola, J., Koskela, T., Lakkala, K., Fioletov, V., Bernhard, G., McKenzie, R., Kondo, Y., O'Neill, M., Slaper, H., den Outer, P., Bais, A. F., and Tamminen, J.: Validation of daily erythemal doses from Ozone Monitoring Instrument with ground based UV measurement data, *J. Geophys. Res.*, 112, D24S44, doi:10.1029/2007JD008830, 2007.
- 15
- WMO (World meteorological Organization): Scientific Assessment of Ozone Depletion: 2014. *Global Ozone Res. Monit. Proj. Rep.* 55, 416 pp., Geneva, Switzerland, 2014.



**Table 1. Monthly and yearly trend values (% per yr.) with 2 sigma errors of estimate (in parentheses) by a standard least-squares regression for the period 1983-2016 (reconstructed and observed data together) and 1996-2016 (only observed data).**

Month	1983-2016	1996-2016
Mar	<b>0.94</b> (0.76)	-0.18(0.45)
Apr	0.48(0.65)	<b>-0.91</b> (0.89)
May	0.15(0.48)	<b>-1.09</b> (0.76)
Jun	0.03(0.52)	<b>-1.18</b> (1.11)
Jul	-0.05(0.55)	-0.15(0.90)
Aug	0.03(0.45)	0.49(0.90)
Sep	0.12(0.38)	0.01(0.79)
Year	0.10(0.36)	-0.61(0.63)



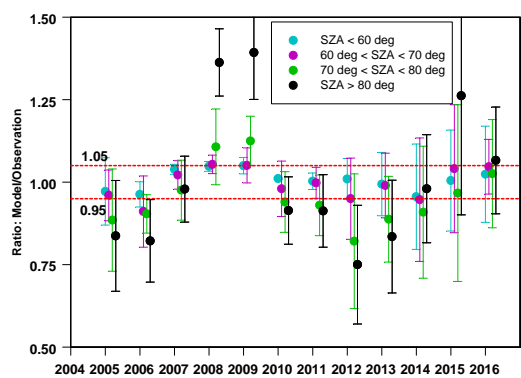
**Figure 1.** The observing platform at the Polish Polar Station Hornsund (77°00'N, 15°33'E). (Photo by P. Sobolewski).

5



5

10



15

Figure 2. The calibration constants for the Kipp and Zonen UVS-AE-T biometer in the period 2005-2016 derived from a comparison of the modeled clear sky doses with the observed ones in cloudless conditions for four solar zenith angle (SZA) ranges



5

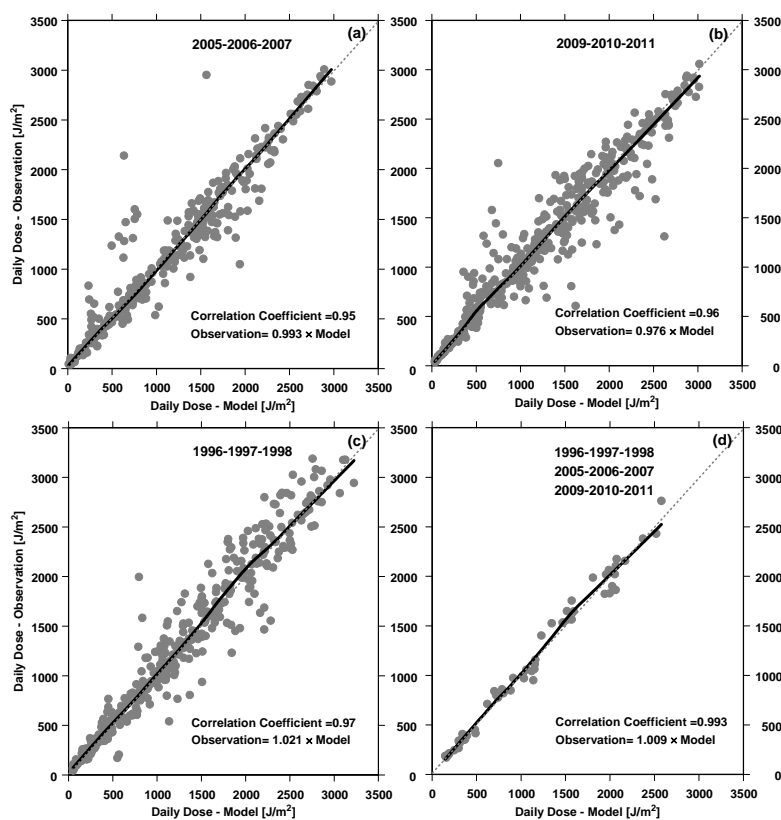


Figure 3. The observed versus modeled erythemal doses: (a) daily doses for the period 2005-2006-2007, (b) daily doses for the period 2009-2010-2011, (c) daily doses for the period 1996-1997-1998, (d) monthly doses for the period 1996-1997-1998, 2005-2006-2007, and 2009-2010-2011.

10

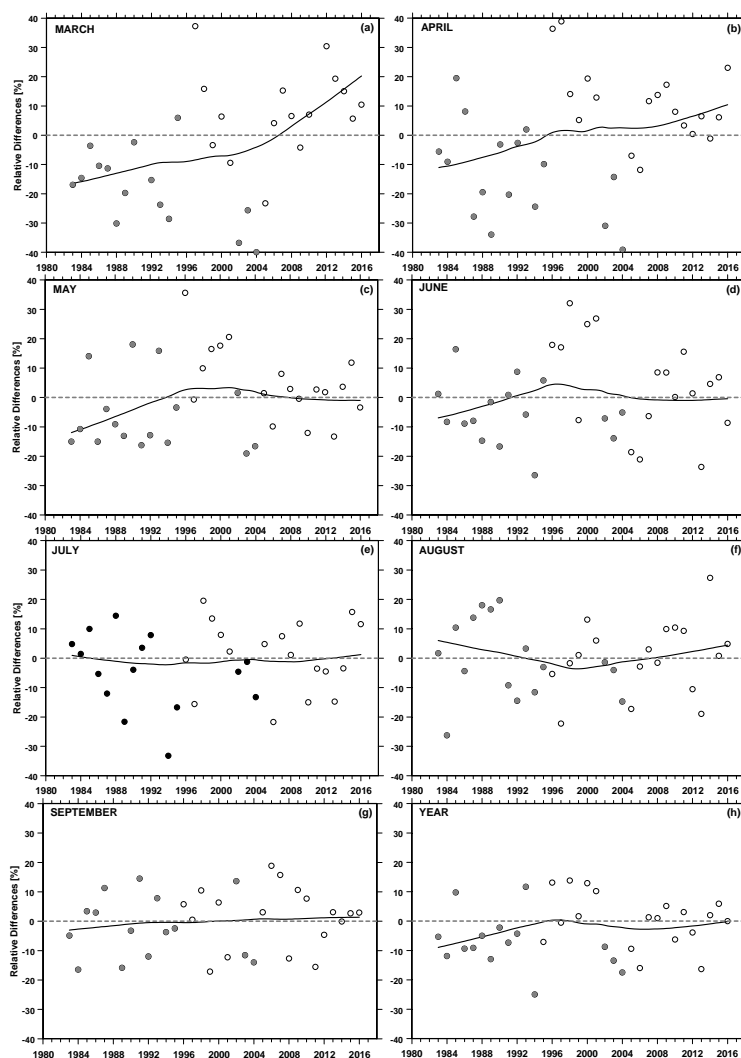


Figure 4. Time series of monthly and yearly fractional deviations of erythemal doses consisting of observed (open circles) and modeled (full circles) data. The solid curve represents the smoothed data by the LOWESS low-pass filter.



5

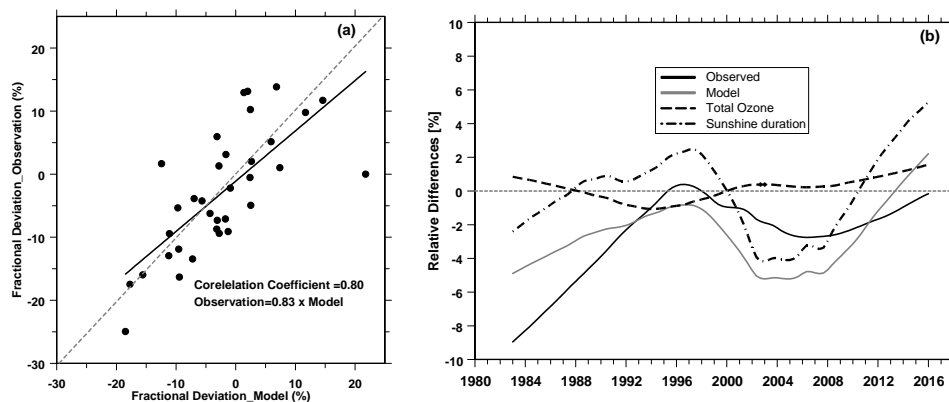
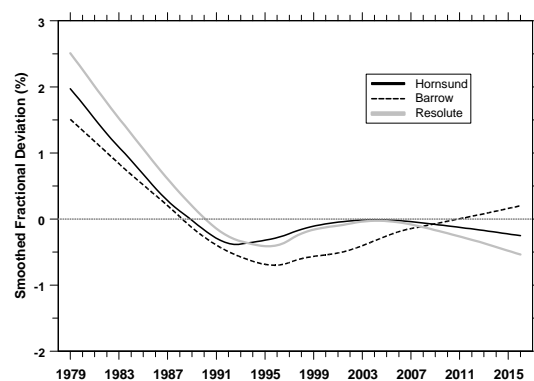


Figure 5. (a) The observed versus modeled yearly erythemal doses (full circles) and the linear regression line, (b) the long-term variability of the yearly data derived by LOWESS smoothing applied to: all (reconstructed +measured) erythemal doses, modeled erythemal doses (based on total ozone and relative sunshine duration), total ozone (by satellite overpasses), and relative sunshine duration (by measurements at the site).

10

15





5

Figure 6. Smoothed time series (1979-2016) of the total ozone fractional deviations at Barrow (Alaska, the United States), Hornsund (Svalbard), and Resolute (Cornwallis Island, Canada) averaged over the period May-June-July-August.

10

15

20

25